

Walter Winter

# Neutrino tomography

Learning about the Earth's interior using the  
propagation of neutrinos

Received:

**Abstract** Because the propagation of neutrinos is affected by the presence of Earth matter, it opens new possibilities to probe the Earth's interior. Different approaches range from techniques based upon the interaction of high energy (above TeV) neutrinos with Earth matter, to methods using the MSW effect on the neutrino oscillations of low energy (MeV to GeV) neutrinos. In principle, neutrinos from many different sources (sun, atmosphere, supernovae, beams etc.) can be used. In this talk, we summarize and compare different approaches with an emphasis on more recent developments. In addition, we point out other geophysical aspects relevant for neutrino oscillations.

**Keywords** Neutrino absorption · Neutrino attenuation · Neutrino oscillations · Matter effects · Neutrino tomography

---

Supported by the W. M. Keck Foundation and NSF grant PHY-0503584.

---

Walter Winter  
Institute for Advanced Study  
School of Natural Sciences  
Einstein Drive  
Princeton, NJ 08540  
E-mail: winter@ias.edu

## 1 Introduction

Neutrinos are elementary particles coming in three active (*i.e.*, weakly interacting) flavors. Since the cross sections for neutrino interactions are very small, neutrinos practically penetrate everything. However, one can compensate for these tiny cross sections by just using enough material in the detector. Depending on neutrino energy and source, the detector has to be protected from backgrounds such that the neutrino events cannot be easily mixed up with different particle interactions. Neutrinos are produced in detectable numbers and with detectable energies by nuclear reactions in the sun, by cosmic ray interactions in the Earth's atmosphere, in nuclear fission reactors, in supernova explosions, in the Earth's crust, and possibly by astrophysical sources. In addition, accelerator-based neutrino sources specifically designed to produce a high-intensity neutrino beam have been successfully operated (such as K2K [6] or MINOS) or are planned. Thus, there are neutrinos from various different sources with different energies.

One of the most recent exciting discoveries in neutrino physics are neutrino oscillations, *i.e.*, neutrinos change flavor while traveling from source to detector. This quantum mechanical phenomenon implies that neutrinos mix, *i.e.*, the eigenstates of the weak interaction are not the same as the mass eigenstates, and at least two out of the three have non-vanishing masses. This is probably the most direct evidence today for physics beyond the standard model of elementary particle physics. Recent neutrino oscillation experiments, especially SNO [1], KamLAND [18], Super-Kamiokande [24], and CHOOZ [7] have helped to quantify this picture. Unlike in quark mixing, two out of the three mixing angles are large, and one is even close to maximal. In addition, the oscillation frequencies have been fairly precisely measured. For one of the mixing angles  $\theta_{13}$ , however, only an upper bound exists, and several parameters (the arrangement of masses, *i.e.*, mass hierarchy, and one complex phase  $\delta_{\text{CP}}$  relevant for neutrino oscillations) are still unknown. Future experiments will probe these parameters starting with the Double Chooz [9], T2K [40], and NO $\nu$ A [11] experiments (for the prospects for the next decade, see, *e.g.*, Ref. [35]).

For neutrino tomography the relevant aspect is the sensitivity to Earth matter. Since it is well known that the cross sections with matter rise at least until 10 TeV [58], the probability of matter interactions can be increased by higher neutrino energies. Neutrino absorption tomography uses this effect to infer on the matter structure. For neutrino oscillations, we know that the so-called MSW matter effect [66; 48; 49] is the most plausible explanation for the solar neutrino deficit [21]. This, however, implies that neutrino oscillation in the Earth have to experience this effect, too. Neutrino oscillation tomography uses the MSW effect to study the matter structure.

## 2 Tomography using the propagation of neutrinos

Tomography using the propagation of neutrinos assumes a neutrino source with a well-known flux and flavor composition, a well-understood neutrino

detector, and a specific neutrino propagation model between source and detector. The key ingredient to any such tomography is a considerable dependence of the propagation model on the matter structure between source and detector. Compared to the detection of geoneutrinos, the object of interest is not the neutrino source, but the material along the baseline (path between source and detector). If the matter structure along the baseline is (partly) unknown, the information from counting neutrino events at different energies by the detector can be used to infer on the matter profile. Two accepted propagation models could be used for neutrino tomography:

**Neutrino absorption:** Because the cross section for neutrino interactions increases proportional to the energy, neutrino interactions lead to attenuation effects. Useful neutrino energies for a significant attenuation are  $E_\nu \gtrsim 1$  TeV.

**Neutrino oscillations:** The MSW effect [66; 48; 49] in neutrino oscillations (coherent forward scattering in matter) leads to a relative phase shift of the electron flavor compared to the muon and tau flavors. This phase shift depends on the electron density. Useful neutrino energies require substantial contributions from the MSW effect as well as large enough oscillation amplitudes. Depending the relevant  $\Delta m^2$ , neutrino energies between 100 MeV and 35 GeV are optimal for studying the Earth's interior.

Beyond these two models, at least small admixtures of non-standard effects have not yet been excluded. Some of these non-standard effects are sensitive to the matter density, too. Examples are mass-varying neutrinos with acceleration couplings to matter fields [43], non-standard neutrino interactions (see Ref. [34] and references therein), and matter-induced (fast) neutrino decay [28]. Because there is not yet any evidence for such effects, we do not include them in this discussion.

Given the above neutrino energies, there are a number of potential sources which could be used for neutrino propagation tomography. For neutrino oscillations, solar neutrinos, supernova neutrinos, atmospheric neutrinos, and neutrino beams (such as superbeams or neutrino factories) are potential sources. For neutrino absorption, high-energy atmospheric neutrinos, a possible high-energy neutrino beam, or cosmic sources are possible sources.

As far as potential geophysics applications are concerned, neutrinos may be interesting for several reasons:

1. Neutrinos propagate on straight lines. The uncertainty in their path (direction) is only as big as the surface area of the detector.
2. Neutrinos are sensitive to complementary quantities to geophysics: Neutrino absorption is directly sensitive to the matter density via the nucleon density. Neutrino oscillations are sensitive to the electron density which can be converted in the matter density by the number of electrons per nucleon (for stable “heavy” materials about two). On the other hand, seismic wave geophysics needs to reconstruct the matter density by the equation of state from the propagation velocity profile.
3. Neutrinos are, in principle, sensitive to the density averaged over the baseline, whereas other geophysics techniques are, in principle, less sensitive towards the innermost parts of the Earth. For example, seismic shear

waves cannot propagate within the outer liquid core, which means that a substantial fraction of the energy deposited in seismic waves is reflected at the mantle-core boundary. Other direct density measurements by the Earth's mass or rotational inertia are less sensitive towards the innermost parts, too, because they measure volume-averaged quantities.

Given these observations, there may be interesting geophysics applications exactly where complementary information is needed. Possible applications range from the detection of density contrasts in the Earth's upper or lower mantle, to the measurement of the average densities of the outer and inner core by independent methods.

### 3 Neutrino absorption tomography

Here we discuss tomography based on attenuation effects in a neutrino flux of high enough energies, which we call, for simplicity, “neutrino absorption tomography”. After we have introduced the principles, we will discuss possible applications with respect to tomography of the whole Earth as well as specific sites.

#### 3.1 Principles

“Neutrino absorption tomography” uses the attenuation of a high-energy neutrino flux as a propagation model. In this case, weak interactions damp the initial flux by the integrated effect of absorption, deflection, and regeneration. For example, muons produced by a muon neutrino interaction are absorbed very quickly in Earth matter, whereas taus produced by tau neutrinos tend to decay before absorption (and some of the decay products are again neutrinos). Only the integrated effect leads to attenuation of the flux. The magnitude of the attenuation effect can be estimated from the cross section

$$\frac{\sigma}{E} \sim 10^{-35} \frac{\text{cm}^2}{\text{TeV}} \quad (1)$$

to be of the order of several per cent over the Earth's diameter for  $E_\nu = 1 \text{ TeV}$ . The interaction cross section rises linearly up to about 10 TeV [58], whereas the behavior above these energies is somewhat more speculative. The energies are usually as high as standard neutrino oscillations do not develop within the Earth. Since the neutrinos interact with nucleons, the attenuation is directly proportional to the nucleon density. Therefore, neutrino absorption is a very directly handle on the matter density with an extremely tiny remaining uncertainty from composition and the difference between neutron and proton mass.

As far as possible potential neutrino sources are concerned, Eq. (1) requires very high neutrino energies. The existence of corresponding neutrino sources is plausible and will be tested by upcoming experiments commonly referred to as “neutrino telescopes”. These neutrino telescopes could also

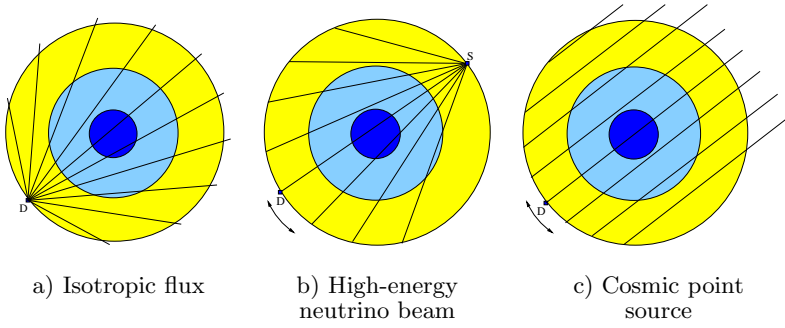


**Fig. 1** Three different approaches to “Whole Earth Tomography” using neutrino absorption. The lines refer to different baselines.

serve as prototypes for the detectors useful for neutrino absorption tomography. The only detected source so far are atmospheric neutrinos produced by the interaction of cosmic rays in the atmosphere. Unfortunately, the atmospheric neutrino flux drops rapidly with energy, which means that statistics is limited at the relevant energies  $E_\nu > 1$  TeV (see, *e.g.*, Ref. [29] for specific values). Other potential candidates include many different possible astrophysics objects, as well as particle physics mechanisms such as decays of dark matter particles. Since we know that the Earth is hit by cosmic rays of very high energies, it might be inferred that astrophysical mechanisms exist which accelerate particles (for example, protons) to these high energies. It is plausible that such mechanisms also produce neutrinos. Potential mechanisms could either produce discrete fluxes from individual objects, or their integrated effect could lead to a diffuse flux over the whole sky. Eventually, one could think about a neutrino beam producing high-energy neutrinos. If, for instance, one used the protons from LHC (7 TeV) to hit a target, the decaying secondaries (pions, kaons) would produce a neutrino flux peaking at about 1 TeV.

### 3.2 Whole Earth tomography

For possible applications of neutrino absorption tomography, there exist two different directions in the literature: Either one could “X-ray” the whole Earth (“Whole Earth tomography”), or one could think about the investigation of specific sites in the Earth’s mantle. We summarize in Fig. 1 different approaches to “Whole Earth tomography”. In case a) (isotropic flux) a neutrino flux from many directions is detected by a detector with good directional resolution. For instance, a possible neutrino source would be a cosmic diffuse flux [42] (related work: Ref. [59]) or the high-energy tail of atmospheric neutrinos (see, *e.g.*, Ref. [29]). This application could be very interesting because it might be available at no additional experimental effort. However, if one wants to study the innermost parts of the Earth, it is (except from sufficient directional resolution and flux isotropy) a major challenge that the fraction

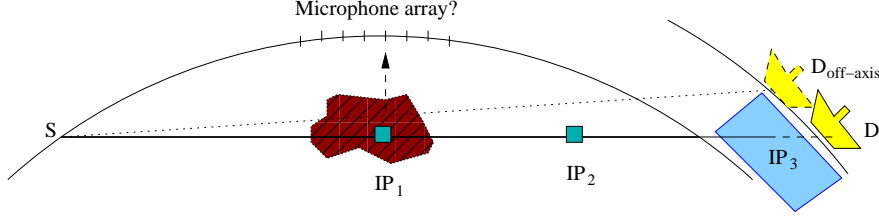


**Fig. 2** Different possibilities for neutrino tomography using a high-energy neutrino beam. The labels “IP” refer to possible interaction points. See text for more details.

of the sky which is seen through the Earth’s inner core is very small ( $\sim 1\%$ ), which means that the statistics for this specific goal is very low. Very good precisions may, on the other hand, be obtained for the mantle (see Fig. 4 of Ref. [42]). In case b) (high-energy neutrino beam) [17; 62; 10; 14; 13] the detector is moved to obtain many baselines, whereas the source is kept fix. In this case, high precisions could be obtained [17]. However, a major challenge might actually be the operation of a high-energy neutrino beam with a moving decay tunnel. Note that such a beam could not only be used for whole Earth tomography, but also for local searches (see below). In case c) (cosmic point source) [62; 45], the flux from a single object is used for the tomography of the Earth. In this case, the flux has to be constant in time to be detected either by a moving detector, or by one detector using many baselines by the rotation of the Earth. Note that the second mechanism cannot be used for the currently largest planned neutrino telescope “IceCube” [2] because it is residing at the south pole.

### 3.3 Specific site tomography

Compared to “whole Earth tomography”, a different direction is the investigation of individual sites, such as in the Earth’s mantle. For example, Ref. [17] extensively reviews techniques based on a high-energy neutrino beam. We summarize some of those in Fig. 2. The neutrinos, produced by the source “S”, may interact at several possible interaction points  $IP$ . If, for example, the site of interest is the dark-shaded cavity, an interaction at  $IP_1$  could create a particle shower leading to sound production, which may be detected by a microphone array at the surface. In addition, the final neutrino flux detected at “D” would be damped depending on the material density in the cavity. An interaction at  $IP_2$  just below the surface ( $\lesssim 200$  m) would produce muons which could still be detected at the surface (such as possibly by a muon detector on a truck). A variation of this flux detected by a moving muon detector could point towards heavy materials. Eventually, a neutrino interaction at  $IP_3$  within the sea water below a muon moving detector would indicate that the initial neutrino has arrived. Since the neutrino energy decreases rapidly by moving the detector out of the beam axis by kinematics, attenuation effects also decrease and the initial flux could be measured by the “off-axis” technology. Comparing this flux to the on-axis flux reveals the

attenuation along the path and therefore some information on the matter structure.

In summary, there are many potential applications of neutrino absorption tomography. The coming years, especially the operation of IceCube, will reveal the possible existence of high-energy cosmic neutrino fluxes. Operating a high-energy neutrino beam may be a major technical challenge, which definitively needs further investigation.

## 4 Neutrino oscillation tomography

In this section, we discuss neutrino tomography using oscillations. First, we introduce the principles of neutrino oscillation tomography: Neutrino oscillations in vacuum and matter, numerical approaches to neutrino oscillation tomography, as well as conceptual (mathematical) problems. Then, we show applications related to solar and supernova neutrinos, and we discuss tomography with neutrino beams.

### 4.1 Principles

Neutrino oscillation tomography uses neutrino oscillations in matter as propagation model. Possible neutrino sources include “natural” ones (*e.g.*, sun, supernova, atmosphere), as well as “man-made” ones (*e.g.*, superbeam,  $\beta$ -beam, neutrino factory). The detection technology depends on the neutrino energy and ranges from Water Cherenkov detectors (lower energies), over liquid scintillators (medium energies), to iron calorimeters (high energies), just to mention some examples.

#### *Neutrino oscillation phenomenon*

Neutrino oscillations are a quantum mechanical phenomenon with two prerequisites: First, the weak interaction eigenstates have to be different from the propagation/mass eigenstates (flavor mixing). Second, the neutrino masses have to be different from each other, which implies that at least two of the active neutrinos have to have non-zero mass [12]. In the limit of two flavors, the flavor transition probability  $\nu_\alpha \rightarrow \nu_\beta$  in vacuum can be written as

$$P_{\alpha\beta} = \sin^2(2\theta) \sin^2\left(\frac{\Delta m^2 L}{4E}\right), \quad (2)$$

where  $\theta$  is the mixing angle of a  $2 \times 2$  rotation matrix  $U$ ,  $\Delta m^2 \equiv m_a^2 - m_b^2$  is the mass-squared difference describing the oscillation frequency,  $L$  is the baseline (distance source-detector), and  $E$  is the neutrino energy. Note that the quotient  $L/E$  determines the oscillation phase. Similarly, the flavor conservation probability  $\nu_\alpha \rightarrow \nu_\alpha$  is given by  $P_{\alpha\alpha} = 1 - P_{\alpha\beta}$  from conservation of unitarity. Practically,  $P_{\alpha\beta}$  is measured as function of  $E$  (convoluted with the neutrino flux and cross sections) for a fixed baseline since the detector cannot be moved. Since we do know that we deal with three active flavors,

the complete picture is somewhat more complicated. Three-flavor neutrino oscillations can be described by six parameters (three mixing angles, one complex phase, and two mass squared differences), which decouple into two-flavor oscillations, described by two parameters each, in certain limits (see Ref. [23] for a recent review). In summary, we have two almost decoupled two-flavor oscillations described by two very different frequencies and large mixing angles, often referred to as “solar” ( $\Delta m_{21}^2$ ,  $\theta_{12}$ ) and “atmospheric” ( $\Delta m_{31}^2$ ,  $\theta_{23}$ ) oscillations. Those could be coupled by  $\theta_{13}$ , for which so far only an upper bound  $\sin^2(2\theta_{13}) \lesssim 0.1$  [7] exists. In addition, we do not yet know anything about the complex phase  $\delta_{\text{CP}}$ , which could lead to sub-leading effects, and the sign of  $\Delta m_{31}^2$  (“mass hierarchy”). These parameters will be probed by neutrino oscillation experiments in the coming years. In this section, we concentrate on the two-flavor case for pedagogical reasons.

### *Matter effects in neutrino oscillations*

Key ingredient to neutrino tomography are matter effects in neutrino oscillations [66; 48; 49]. Since Earth matter contains plenty of electrons, but no muons or taus, charged-current interactions of the electron neutrino flavor through coherent forward scattering lead to a relative phase shift compared to the muon and tau neutrino flavors. In the Hamiltonian in two flavors, the matter term enters as the second term in

$$\mathcal{H}(n_e) = U \begin{pmatrix} 0 & 0 \\ 0 & \frac{\Delta m_{21}^2}{2E} \end{pmatrix} U^\dagger + \begin{pmatrix} A(n_e) & 0 \\ 0 & 0 \end{pmatrix} \quad (3)$$

in flavor space, where  $A(n_e) = \pm\sqrt{2}G_F n_e$  is the matter potential as function of the electron density  $n_e$  and the coupling constant  $G_F$ , and the different signs refer to neutrinos (plus) and antineutrinos (minus). Assuming that the number of electrons per nucleon is approximately 0.5 for stable “heavy” (considerably heavier than hydrogen) materials, the electron density can be converted into the matter density as  $n_e = 0.5 \rho / m_N$  with  $m_N$  the nucleon mass. In this case, there is some material dependence of this factor 0.5 (“electron fraction”), which, however, might also be used to obtain additional information on the composition. In two flavors and for constant matter density, Eq. (2) can be easily re-written by a parameter mapping between vacuum and matter parameters:

$$P_{\alpha\beta} = \sin^2(2\tilde{\theta}) \sin^2\left(\frac{\Delta\tilde{m}^2 L}{4E}\right), \quad (4)$$

where

$$\Delta\tilde{m}^2 = \xi \cdot \Delta m^2, \quad \sin(2\tilde{\theta}) = \frac{\sin(2\theta)}{\xi}, \quad (5)$$

with

$$\xi \equiv \sqrt{\sin^2(2\theta) + (\cos(2\theta) - \hat{A})^2}, \quad (6)$$

$$\hat{A} \equiv \frac{2\sqrt{2}G_F n_e E}{\Delta m^2}. \quad (7)$$



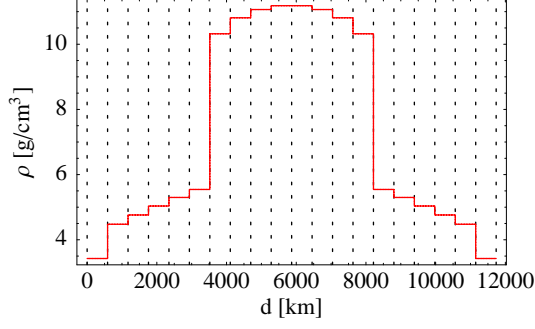


**Fig. 3** Example for a REM- (“Reference Earth Model”) based matter density profile for a baseline of 12 000 km as used for the numerical evaluation of the neutrino propagation (20 steps). The matter density within each layer is assumed to be constant.

One can easily read off these formulas that for  $\hat{A} \rightarrow \cos(2\theta)$  the parameter  $\xi$  in Eq. (6) becomes minimal, which means that the oscillation frequency in matter becomes minimal and the effective mixing maximal (*cf.*, Eq. (5)). This case is often referred to as “matter resonance”, where the condition  $\hat{A} \rightarrow \cos(2\theta)$  evaluates to

$$E_{\text{res}} \sim 13\,200 \cos(2\theta) \frac{\Delta m^2 [\text{eV}^2]}{\rho [\text{g}/\text{cm}^3]}. \quad (8)$$

This condition together with the requirement of a large oscillation phase  $\sin^2(\Delta m^2 L/(4E)) = \mathcal{O}(1)$  leads to the “ideal” energies for neutrino oscillation tomography depending on the considered  $\Delta m^2$ :

$$\begin{aligned} \Delta m_{21}^2 : E &\sim 100 \text{ MeV to } 1 \text{ GeV}, \\ \Delta m_{31}^2 : E &\sim \text{few GeV to } 35 \text{ GeV}. \end{aligned}$$

If the neutrino energy is far out of this range, either the matter effects or the overall event rate from oscillations will be strongly suppressed. However, there are also possible applications. Since, for instance, for solar neutrinos  $E \ll E_{\text{res}}$ , one can use the absence of the resonance for analytical simplifications, as we will discuss later.

#### *Numerical evaluation and conceptual problems*

In order to numerically study neutrino oscillation tomography, a commonly used method is the “evolution operator method” (*cf.*, *e.g.*, Ref. [52]). This method assumes that the matter density profile be discretized into layers with constant density (*cf.*, Fig. 3 for an example). The initial state  $|\nu_\alpha\rangle$  is then propagated through the different matter density layers with depths  $x_j$  with the evolution operators

$$\mathcal{V}(x_j, \rho_j) = e^{-i\mathcal{H}(\rho_j)x_j} \quad (9)$$

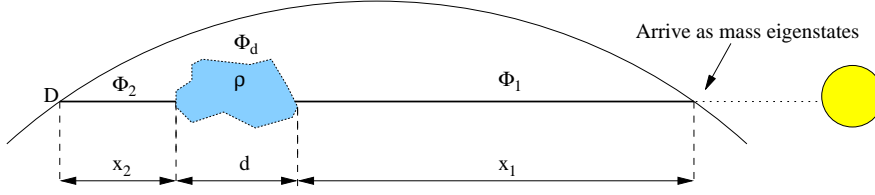


**Fig. 4** Neutrino oscillation tomography using solar neutrinos for the investigation of a cavity in the Earth's mantle.

while the Hamiltonian within each layer  $\mathcal{H}$  (*cf.*, Eq. (3)) is assumed to have no explicit time-independence (it is given in constant density  $\rho_j$ ). The transition probability is then obtained as

$$P_{\alpha\beta} = |\langle \nu_\beta | \mathcal{V}(x_n, \rho_n) \dots \mathcal{V}(x_1, \rho_1) | \nu_\alpha \rangle|^2. \quad (10)$$

In practice, Eq. (10) is evaluated by diagonalizing the Hamiltonian for each density step, *i.e.*, by calculating the mass eigenstates in each matter layer. Note that in general

$$[\mathcal{V}(x_i, \rho_i), \mathcal{V}(x_j, \rho_j)] \neq 0 \quad \text{for} \quad \rho_i \neq \rho_j, \quad (11)$$

which means that the evolution operators of different layers do not necessarily commute. This already implies that the information from a single baseline must be somehow sensitive towards the arrangement of the matter density layers. This is very different from X-ray or neutrino absorption tomography which do not have positional information from one baseline.

An important conceptual problem in neutrino oscillation tomography is the matter profile inversion problem [19; 20]. Assume that a matter density profile such as in Fig. 3 is given. For a specific experiment setup, it is then fairly easy to compute the corresponding transition probabilities or event rates as function of energy. However, the reverse problem is theoretically generally unsolved: Assume that the transition probability is known up to infinite energies, then it would be very useful to be able to compute the matter profile from that. So far, there have been several attempts to solve this problem using simplifications, such as

- Simple models using only very few discrete steps (see, *e.g.*, Refs. [50; 51; 54])
- Linearization in a low density medium (solar, supernova neutrinos) [4]
- Discretization of a more complex profile using non-deterministic algorithms to fit a large number of parameters [53].

Below, we will discuss some of these approaches in greater detail.

#### 4.2 Neutrino oscillation tomography with solar and supernova neutrinos

Solar and supernova neutrinos are theoretically very interesting for neutrino tomography because matter effects are introduced off the resonance in Earth

matter, *i.e.*, the neutrino energy  $E \ll E_{\text{res}}$  (*cf.*, Eq. (8) for  $\Delta m^2 = \Delta m_{21}^2$ ), or equivalently  $\hat{A} \ll 1$ . This means that one does not expect strong matter effects in Earth matter as opposed to within the sun. However, this limit is theoretically very useful to study tomography because it allows for perturbation theory and other simplified approaches. It is often referred to as neutrino oscillations in a “low density medium” [38; 39] because the density in the Earth is much lower than in the sun.

### *Detecting a cavity*

We show in Fig. 4 a possible setup for neutrino tomography using solar neutrinos following Ref. [37]. In this setup, the detector is fixed while the Earth is rotating, which means that the cavity with density  $\rho$  is “exposed” (in line of sight sun-detector) a time  $0 < t_{\text{exp}} < 24$  hr per day. The change in the oscillation probability during this time is, depending on geometry and density contrast,  $\lesssim 0.1\%$ . This leads to a required detector mass  $M \gtrsim 130 \text{ Mt}/(t_{\text{exp}}[\text{hr}])$ , which has a lower limit of 5 Mt at the poles. Thus, from the statistics point of view, this approach is very challenging, and backgrounds might be an important issue. In addition, for such large detectors, the detector surface area might be of the order of the cavity size. There are, however, interesting theoretical results from such a discussion. Let us define the oscillation phases in the individual steps  $x_1$ ,  $d$ , and  $x_2$  as [37]

$$\Phi_i \equiv \frac{\Delta m_{21}^2 x_i}{2E} \sqrt{\sin^2 2\theta_{12} + (\cos 2\theta - \hat{A}_i)^2} \quad (12)$$

with the corresponding matter potentials  $\hat{A}_i$  (*cf.*, Fig. 4). One can show that if mass eigenstates arrive at the surface of the Earth (solar and supernova neutrinos), the change in probability  $\Delta P$  (cavity exposed-not exposed) only depends on  $\Phi_2$ , but not on  $\Phi_1$ . In addition, there is a damping of contributions from remote distances  $x_2$ , which means that solar neutrinos are less sensitive to the deep interior of the Earth than to structures close to the detector.

### *Matter density inversion problem*

A further application of the low density limit is to theoretically solve the matter profile inversion problem. Following Ref. [4], the Earth matter effect on solar or supernova neutrinos is fully encoded in the quantity (“day-night regeneration effect”)

$$P_{2e}^{\text{night}} - P_{2e}^{\text{day}} = \frac{1}{2} \cos^2 \theta_{13} \sin^2 2\theta_{12} f(\delta) \quad (13)$$

with

$$f(\delta) = \int_0^L dx A(x) \sin \left[ 2 \int_x^L \omega(x') dx' \right], \quad (14)$$

$$\omega(x) = \sqrt{(\delta \cos 2\theta_{12} - A(x)/2)^2 + \delta^2 \sin^2 2\theta_{12}}, \quad (15)$$

$$A(x) = \sqrt{2} G_F n_e(x), \quad \delta \equiv \frac{\Delta m_{21}^2}{4E}. \quad (16)$$

This implies that the measured quantity is  $f(\delta)$ , *i.e.*, a function of energy, which needs to be inverted into the matter profile  $A(x)$ . Especially, the double integral in Eq. (14) is quite complicated to invert. However, using the low density limit  $A \ll 2\delta$  (or equivalently  $\hat{A} \ll 1$ ) as well as  $AL \ll 1$  ( $L \ll 1700$  km), one can linearize Eq. (14) in order to obtain

$$f(\delta) = \int_0^L dx A(x) \sin[2\delta(L-x)]. \quad (17)$$

This is just the Fourier transform of the matter density profile, *i.e.*,

$$A(x) = \frac{4}{\pi} \int_0^\infty f(\delta) \sin(2\delta(L-x)) d\delta, \quad (18)$$

and the matter density profile inversion problem is solved. One problem is very obvious from Eq. (18): One needs to know  $f(\delta)$  in the whole interval  $0 \leq E \leq \infty$  which is practically impossible. The authors of Ref. [4] suggest an iteration method to solve this problem. Additional challenges are statistics and a finite energy resolution, which is “washing out” the edges in the profile. One interesting advantage of using solar or supernova neutrinos is the sensitivity to asymmetric profiles, *i.e.*, for mass-flavor oscillations there is no degeneracy between one profile and the time-inverted version, which otherwise (for flavor-flavor oscillations) can only be resolved by suppressed three-flavor effects.

#### *Supernova neutrinos to spy on the Earth’s core*

Unlike solar neutrinos, which are limited to energies below 20 MeV, supernova neutrinos from a possible galactic supernova explosion have a high-energy tail which is closer to the Earth matter resonance energy. This effect is illustrated in Fig. 5 (right) which compares the energy spectrum between two Super-Kamiokande-like detectors with and without Earth matter effects. It is obvious from this figure that the difference between the spectra around the peak at  $\sim 20$  MeV is tiny, whereas statistically significant deviations can be found at larger energies. Such a scenario could happen if supernova neutrinos were detected by two similar-sized detectors, one on the Earth’s surface and with the Earth’s core in the line of sight (*cf.*, Fig. 5, left). Note that the

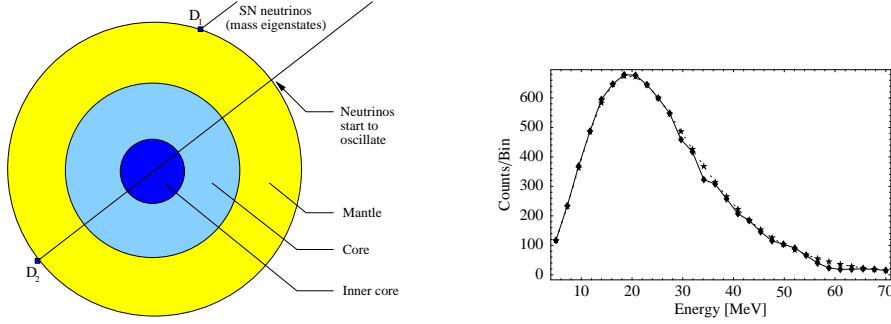


**Fig. 5** Illustration for the tomography of the Earth’s core using supernova neutrinos (left) and difference between the event rate spectra (electron antineutrinos) of  $D_1$  and  $D_2$  for Super-Kamiokande-like detectors (right). The difference between these spectra corresponds to  $\Delta\chi^2 \simeq 35$  for the Earth matter effects, *i.e.*, it is highly significant. Figures from Ref. [46].

supernova neutrinos are detected within a very short time frame  $\ll 24$  hr, which means that one would actually obtain a “snapshot” of the Earth’s interior. As it has been demonstrated in Ref. [46], for a galactic supernova in the distance  $D = 10$  kpc with an energy release of  $E = 3 \cdot 10^{53}$  ergs, two megaton-size Water Cherenkov detectors could measure the density of the Earth’s core at the per cent level with a number of challenges: First, the Earth’s mantle density is assumed to be known at the 2% level. Second, the solar oscillation parameters have to be known at the 0.2% level. Third, too similar supernova fluxes for the different flavors (similar temperatures) and deviations from energy equipartition are unfavorable. And fourth, one has to have some knowledge on the flavor composition of the flux, possibly from detection of different flavors.

#### 4.3 Neutrino oscillation tomography with neutrino beams

We now discuss neutrino oscillation tomography with the “man-made” neutrino beams. Neutrino beams are planned or future neutrino sources using accelerators, where the neutrino beam is produced by pion/kaon decays (superbeams, see, *e.g.*, Refs. [40; 11]), by muon decays (neutrino factory, see, *e.g.*, Refs. [25; 8; 5]), or by the decay of unstable nuclei ( $\beta$ -Beam, see, *e.g.*, Refs. [67; 15; 16; 36]). Neutrino beams have, compared to “natural” neutrino sources, the advantage that either flux and flavor composition are well-known, or a near detector can be used to improve the knowledge on these quantities as well as on the interaction cross sections. There is, however, one major obstacle common to all of these experiments: Matter effects especially enter in the  $\nu_e \leftrightarrow \nu_\mu$  flavor transition which is suppressed by the small mixing angle  $\sin^2(2\theta_{13})$ . Up to now, this mixing angle is unknown and only an upper bound exists [7]. Experiments within the coming ten years will reveal if  $\sin^2(2\theta_{13})$  is suitably large for the applications discussed here (for a summary, see, *e.g.*, Ref. [35]). Therefore, the experiment performance has always to be

evaluated as function of  $\sin^2(2\theta_{13})$ . In this section, we split the discussion into conceptual areas linked to tomography with neutrino beams.

#### *Positional information for a single baseline*

An interesting question is discussed in Ref. [54]: Assume we have a beam crossing a cavity with a specific density contrast compared to the surrounding matter. Then one wants to know

- How large has the cavity to be to be detected?
- Can the position of the cavity be measured and if so, how precisely?

In Ref. [54] a 500 MeV superbeam is assumed with very luminous 200 000 events in total. The density in the cavity is assumed to be  $1 \text{ g/cm}^3$  (water), the baseline  $L = 1\,000 \text{ km}$ , and  $\sin^2(2\theta_{13}) = 0.03$ , where a smaller number of events can be compensated by a larger  $\sin^2(2\theta_{13})$ . It turns out that the cavity has to be longer than about 100 km to be found and its size can be measured to about  $\pm 50 \text{ km}$ . As most important result, the position of the cavity can be reconstructed  $\pm 100 \text{ km}$  from a single baseline, which is very different from X-ray or absorption tomography. However, there is a degeneracy in the position between  $x$  and  $L - x$  which can be only resolved by suppressed three-flavor effects. This example demonstrates already one of the basic principles of neutrino oscillation tomography: Positional information is available already from a single baseline.

#### *Resolution of structures and edges*

One can learn about the resolution of structures and edges from the numerical solution of the matter density inversion problem. In Ref. [53] a (symmetrized) REM profile is reconstructed from a single baseline crossing the outer core with 14 degrees of freedom using a genetic algorithm. Naturally, there are many degenerate profiles close to the  $1\sigma$ ,  $2\sigma$ , and  $3\sigma$  contours, and one cannot show a contour in 14-dimensional parameter space. Therefore, we show in Fig. 6 several “typical” representatives close to the  $1\sigma$ ,  $2\sigma$ , and  $3\sigma$  contours for a neutrino factory, where the total number of oscillated events is for  $\sin^2(2\theta_{13}) = 0.1$  only about a factor of four above currently discussed luminosities (see, *e.g.*, Ref. [33]). From Fig. 6, one can easily read off that such an experiment could, in principle, reconstruct the mantle-core-mantle structure of the Earth. However, structures smaller than several hundred kilometers cannot be resolved. In addition, the mantle-core boundary cannot be resolved at a sufficiently high confidence level from a single baseline. Analytically, it has been demonstrated in Ref. [53] that structures much smaller than the oscillation length in matter cannot be resolved – as one would naturally expect similar to other quantum mechanical phenomena. In conclusion, neutrino oscillations in matter are very sensitive towards average densities and the arrangement of structure on the length scale of the oscillation length. However, neither can edges nor small structures be precisely resolved.

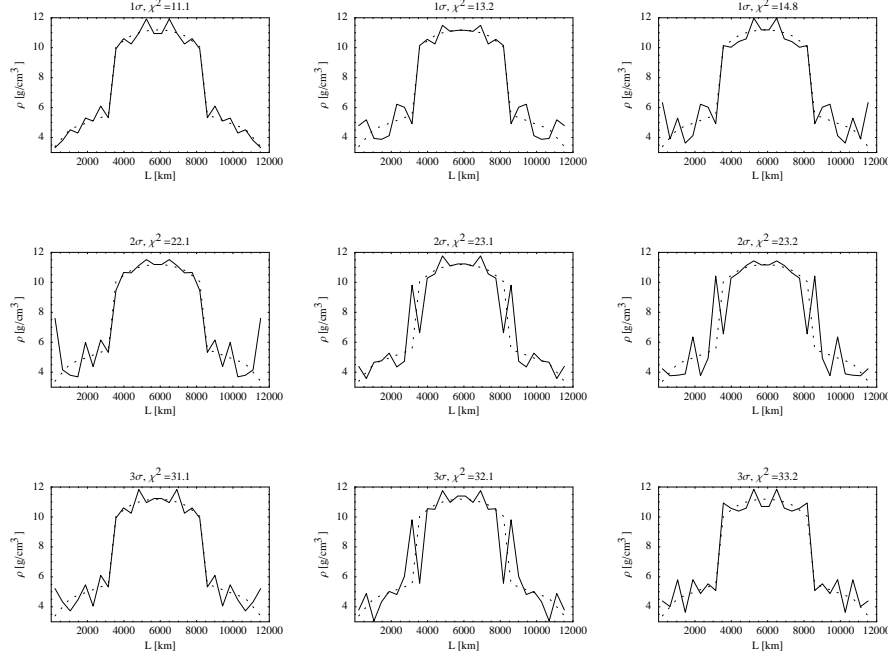


**Fig. 6** Examples for reconstructed (symmetric) REM profiles from an extremely luminous neutrino factory close to the  $1\sigma$  (upper row),  $2\sigma$  (middle row), and  $3\sigma$  (lower row) contours for  $L = 11\,736$  km (14 d.o.f.). Figure from Ref. [53].

### Density measurement

Since we know that neutrino oscillations measure more or less the baseline-averaged densities  $\bar{\rho}_i^L = 1/L \int_0^L \tilde{\rho}(l) dl$  over long distances plus some suppressed interference effects, we can use this to discuss possible applications. For example, let us assume that we want to perform a simple one-parameter measurement of the Earth's inner core density. Because the Earth's mass is fixed, we need to correct the average mantle or outer core density for any shift of the inner core density. Note, however, that it is the volume-averaged density to be corrected, which means that large shifts in the Earth's inner core density cause only very small density corrections in the mantle. This example illustrates already one potential strength of neutrino oscillation tomography: Since a neutrinos from a “vertical” baseline travel similar distances in mantle, core, and inner core, there should be no *a priori* disadvantage for the innermost parts of the Earth. In Ref. [65] a neutrino factory setup from Ref. [33] with currently anticipated luminosities was chosen to test this hypothesis for realistic statistics. In order to measure the oscillation parameters, the experiment with  $L = 2 R_E$  was combined with a  $L = 3\,000$  km. The precision of the measurement can be found in Fig. 7 as function of  $\sin^2(2\theta_{13})$ . One case easily read off that a per cent level measurement is realistic for  $\sin^2(2\theta_{13}) \gtrsim 0.01$ . Most importantly, the application survives the unknown

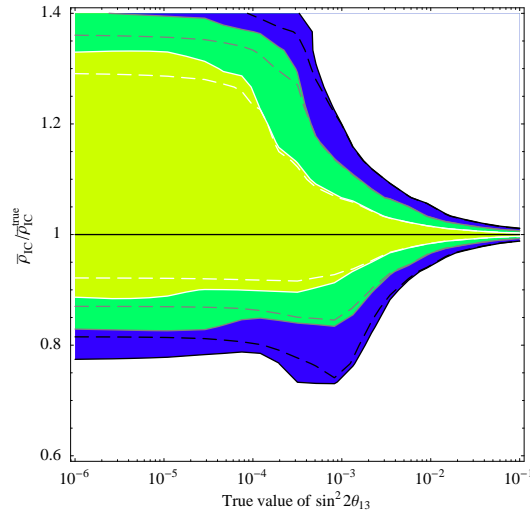


**Fig. 7** The measurement of  $\bar{\rho}_{IC}$  (inner core density) as function of the true value of  $\sin^2(2\theta_{13})$  at the  $1\sigma$ ,  $2\sigma$ , and  $3\sigma$  confidence levels (from light to dark shaded regions). For the baselines,  $L = 2 \cdot R_E$  combined with a shorter baseline  $L = 3000$  km to reduce correlations is used. The dashed curves correspond to fixing the oscillation parameters, *i.e.*, to not taking into account correlations and degeneracies. Figure from Ref. [65].

oscillation parameters and the performance is already close to the optimum (dashed curves). For smaller values of  $0.001 \lesssim \sin^2(2\theta_{13}) \lesssim 0.01$ , the correlations would be much worse without the  $L = 3000$  km baseline. For large values of  $\sin^2(2\theta_{13}) \gtrsim 0.01$ , the vertical baseline alone is hardly affected by correlations with the oscillation parameters: As illustrated in Ref. [64], CP effects are suppressed for very long baselines. Since there is only a number of potential high-energy laboratories around the world which could host a neutrino factory, we show in Fig. 8 some examples and the corresponding outer and inner core crossing baselines. Obviously, there are potential detector locations for some of the laboratories, which are, however, not exactly on the  $L = 2R_E$ -axis. Relaxing this baseline constraint somewhat, one can show that one can find detector locations for a small drop in precision [65]. In summary, this application illustrates that a density measurement could be performed with a) reasonable statistics, b) including the correlations with the oscillation parameters, and c) reasonably small values of  $\sin^2(2\theta_{13})$ . In the future, it has to be clarified how large the additional effort for such a facility (the vertical storage ring) would be. Note, however, that there are plenty of other applications of a “very long” neutrino factory baseline, such as the “magic baseline” to resolve degeneracies [32] ( $L \sim 7500$  km), the test of the MSW effect for  $\sin^2(2\theta_{13}) = 0$  [63] ( $L \gtrsim 5500$  km), the mass hierarchy measurement for  $\sin^2(2\theta_{13}) = 0$  [31; 30] ( $L \sim 6000$  km), and the test of the “parametric resonance” [3; 57] ( $L \gg 10665$  km).



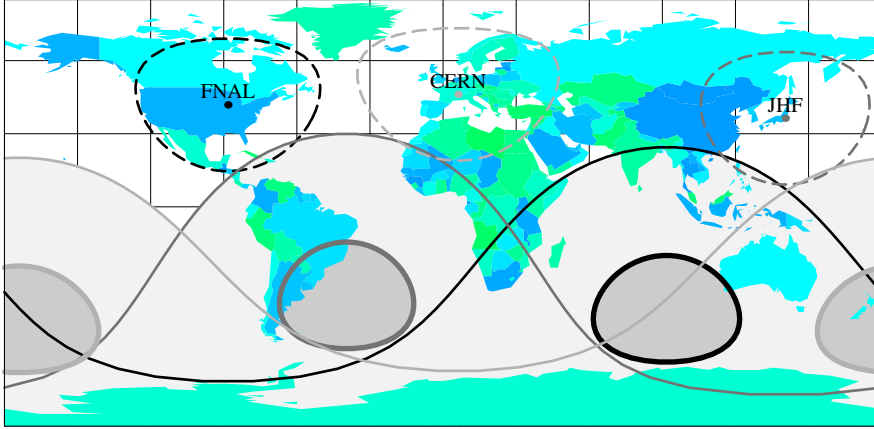


**Fig. 8** Positions of three of the major potential neutrino factory laboratories, (typical)  $L = 3000$  km detector sites (dashed curves), as well as potential detector sites with outer core crossing baselines (below thin solid curves), and inner core crossing baselines (within thick solid curves). The colors of the curves represent the different laboratories. Figure from Ref. [65].

In addition to the described neutrino sources, note that tomography comparing the neutrino and antineutrino disappearance information from atmospheric neutrinos might, in principle, be possible as well [26].

## 5 Other geophysical aspects of neutrino oscillations

It is well known that matter density uncertainties spoil the extraction of the oscillation parameters from the measurements (see Refs. [41; 27; 60; 22; 56; 61; 44; 55] and references therein). In particular for baselines sensitive  $\delta_{\text{CP}}$ , such as  $L \sim 3000$  km at a neutrino factory, the additional correlation with the matter density affects the precision measurements of  $\sin^2(2\theta_{13})$  and  $\delta_{\text{CP}}$ , and the CP violation sensitivity. This effect is illustrated in Fig. 9 for the precision of  $\delta_{\text{CP}}$  and different matter density uncertainties  $\Delta\rho^*$ . Especially for large  $\sin^2(2\theta_{13})$ , any uncertainty larger than about 1% affects the precision severely. Note that the baseline used for Fig. 9 is  $L = 3000$  km, which means that the neutrinos travel in an average depth of  $\sim 120$  km up to a maximum depth of  $\sim 180$  km. In these depths, the uncertainty among geophysics models is currently at the level of 5% [27]. Since the matter density uncertainties may affect the competitiveness of a neutrino factory with a superbeam (operated at shorter baselines) for large values of  $\sin^2(2\theta_{13})$ , improved knowledge for specifically chosen baselines would be very helpful.

## 6 Summary and conclusions

In summary, neutrino tomography might be a very complementary approach to geophysical methods. For example, neutrinos travel on straight lines with

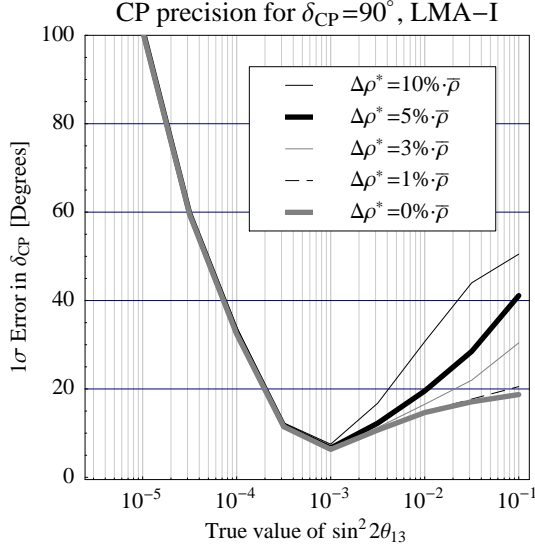


**Fig. 9** The precision of the measurement of  $\delta_{\text{CP}}$  for a neutrino factory and the simulated value  $\delta_{\text{CP}} = 90^\circ$  as a function of the true value of  $\sin^2(2\theta_{13})$  at the  $1\sigma$  confidence level. The different curves correspond to different allowed matter density uncertainties  $\Delta\rho^*$  as described in the plot legend, especially the thick curves correspond to no matter density uncertainty (light thick curve) and the often used uncertainty  $\Delta\rho^* = 5\% \cdot \bar{\rho}$  (dark thick curve). Figure from Ref. [55].

almost no uncertainty in their path. Furthermore, neutrino tomography is either sensitive to the nucleon density (absorption tomography) or electron density (oscillation tomography). In comparison, the paths of seismic waves are curved, and there is some uncertainty in them. In addition, the matter density has to be reconstructed from the propagation velocity profile by the equation of state. This means that neutrino tomography might be a more “direct” handle on the matter density and could be very useful to investigate specifically localized regions, such as in the lower mantle. Moreover, there is no principle reason to prevent neutrinos from penetrating the Earth’s core, whereas seismic waves are partially reflected at the mantle-core and outer-inner core boundaries. Note that though the most precise information on deviations from the REM (“Reference Earth Model”) in the Earth’s mantle comes from seismic waves, there are other geophysical methods which might be more directly sensitive towards the matter density, such as normal modes, mass, and rotational inertia of the Earth. Nevertheless, none of those could provide a measurement along a very specific path.

The main challenges for neutrino tomography might be the existence of high-energy neutrino sources for absorption tomography, and the statistics for oscillation tomography. For example, neutrino oscillation tomography could, in principle, reconstruct the matter density profile along a single baseline due to interference effects among different matter density layers. Note, however, that neutrino oscillations are to first order sensitive towards densities

averaged over the scale of the oscillation length, which means that such sophisticated applications require extremely large luminosities (detector mass  $\times$  source power  $\times$  running time) and might be very challenging. On the other hand, very simple questions, such as a one-parameter measurement of the average density along the path or the discrimination between to very specific degenerate geophysical models might be feasible within the next decades. For example, the achievable precision for the inner core density of the Earth with a neutrino factory experiment might be quite comparable ( $\pm 0.23 \text{ g/cm}^3$  for  $\sin^2(2\theta_{13}) = 0.01$  and  $\pm 0.06 \text{ g/cm}^3$  for  $\sin^2(2\theta_{13}) = 0.1$  [65]) to current precisions given for the density jump at the inner-core boundary from geophysics (*e.g.*,  $\pm 0.18 \text{ g/cm}^3$  in Ref. [47]). We therefore conclude that it will be important that the right and simple questions to be asked by discussions between neutrino physicists and geophysicists.

**Acknowledgements** I would like to thank Evgeny Akhmedov, Tommy Ohlsson, and Kris Sigurdson for useful comments and discussions. In addition, I would like to thanks the organizers of the workshop “Neutrino Sciences 2005: Neutrino geophysics” for an excellent workshop with vivid discussions.

## References

1. Ahmad QR, et al (2002) Direct evidence for neutrino flavor transformation from neutral-current interactions in the Sudbury Neutrino Observatory. Phys Rev Lett 89:011,301, [nucl-ex/0204008](#)
2. Ahrens J, et al (2004) Sensitivity of the IceCube detector to astrophysical sources of high energy muon neutrinos. Astropart Phys 20:507–532, [astro-ph/0305196](#)
3. Akhmedov EK (1999) Parametric resonance of neutrino oscillations and passage of solar and atmospheric neutrinos through the earth. Nucl Phys B538:25–51, [hep-ph/9805272](#)
4. Akhmedov EK, Tortola MA, Valle JWF (2005) Geotomography with solar and supernova neutrinos. JHEP 06:053, [hep-ph/0502154](#)
5. Albright C, et al (2004) The neutrino factory and beta beam experiments and development [physics/0411123](#)
6. Aliu E, et al (2005) Evidence for muon neutrino oscillation in an accelerator-based experiment. Phys Rev Lett 94:081,802, [hep-ex/0411038](#)
7. Apollonio M, et al (1999) Limits on neutrino oscillations from the CHOOZ experiment. Phys Lett B466:415–430, [hep-ex/9907037](#)
8. Apollonio M, et al (2002) Oscillation physics with a neutrino factory. [hep-ph/0210192](#)
9. Ardellier F, et al (2004) Letter of intent for Double-CHOOZ: A search for the mixing angle  $\theta_{13}$  [hep-ex/0405032](#)
10. Askar’yan GA (1984) Investigation of the earth by means of neutrinos. Neutrino geology. Usp Fiz Nauk 144:523–530, [Sov. Phys. Usp. 27 (1984) 896]
11. Ayres DS, et al (2004) NOvA proposal to build a 30-kiloton off-axis detector to study neutrino oscillations in the Fermilab NuMI beamline [hep-ex/0503053](#)
12. Bilenky SM, Pontecorvo B (1978) Lepton mixing and neutrino oscillations. Phys Rept 41:225–261
13. Borisov AB, Dolgoshein BA (1993) Determination of rock density by means of high-energy neutrino beams by the delayed muon method. Phys Atom Nucl 56:755–761
14. Borisov AB, Dolgoshein BA, Kalinovskiy AN (1986) Direct method for determination of differential distribution of the earth density by means of high-energy neutrino scattering. (in Russian). Yad Fiz 44:681–689

15. Bouchez J, Lindroos M, Mezzetto M (2004) Beta beams: Present design and expected performances. AIP Conf Proc 721:37–47, [hep-ex/0310059](#)
16. Burguet-Castell J, Casper D, Gomez-Cadenas JJ, Hernandez P, Sanchez F (2004) Neutrino oscillation physics with a higher gamma beta-beam. Nucl Phys B695:217–240, [hep-ph/0312068](#)
17. De Rujula A, Glashow SL, Wilson RR, Charpak G (1983) Neutrino exploration of the earth. Phys Rept 99:341
18. Eguchi K, et al (2003) First results from kamland: Evidence for reactor anti-neutrino disappearance. Phys Rev Lett 90:021,802, [hep-ex/0212021](#)
19. Ermilova VK, Tsarev VA, Chechin VA (1986) Buildup of neutrino oscillations in the earth. Pis'ma Zh Eksp Teor Fiz 43:353, [JETP Lett. 43 (1986) 453]
20. Ermilova VK, Tsarev VA, Chechin VA (1988) Restoration of the density distribution of material based on neutrino oscillations. Bull Lebedev Phys Inst NO.3:51
21. Fogli G, Lisi E (2004) Evidence for the MSW effect. New J Phys 6:139
22. Fogli GL, Lettera G, Lisi E (2001) Effects of matter density variations on dominant oscillations in long baseline neutrino experiments [hep-ph/0112241](#)
23. Fogli GL, Lisi E, Marrone A, Palazzo A (2005) Global analysis of three-flavor neutrino masses and mixings [hep-ph/0506083](#)
24. Fukuda Y, et al (1998) Evidence for oscillation of atmospheric neutrinos. Phys Rev Lett 81:1562–1567, [hep-ex/9807003](#)
25. Geer S (1998) Neutrino beams from muon storage rings: Characteristics and physics potential. Phys Rev D57:6989–6997
26. Geiser A, Kahle B (2002) Tomography of the earth by the oscillation of atmospheric neutrinos: A study of principle. Poster presented at Neutrino 2002 Munich
27. Geller RJ, Hara T (2001) Geophysical aspects of very long baseline neutrino experiments. Nucl Instrum Meth A503:187–191, [hep-ph/0111342](#)
28. Giunti C, Kim CW, Lee UW, Lam WP (1992) Majoron decay of neutrinos in matter. Phys Rev D45:1557–1568
29. Gonzalez-Garcia MC, Halzen F, Maltoni M (2005) Physics reach of high-energy and high-statistics Icecube atmospheric neutrino data. Phys Rev D71:093,010, [hep-ph/0502223](#)
30. de Gouvea A, Winter W (2005) What would it take to determine the neutrino mass hierarchy if  $\theta_{13}$  were too small? Phys Rev D (to be published), [hep-ph/0509359](#)
31. de Gouvea A, Jenkins J, Kayser B (2005) Neutrino mass hierarchy, vacuum oscillations, and vanishing  $\theta_{13}$  [hep-ph/0503079](#)
32. Huber P, Winter W (2003) Neutrino factories and the 'magic' baseline. Phys Rev D68:037,301, [hep-ph/0301257](#)
33. Huber P, Lindner M, Winter W (2002) Superbeams versus neutrino factories. Nucl Phys B645:3–48, [hep-ph/0204352](#)
34. Huber P, Schwetz T, Valle JWF (2002) Confusing non-standard neutrino interactions with oscillations at a neutrino factory. Phys Rev D66:013,006, [hep-ph/0202048](#)
35. Huber P, Lindner M, Rolinec M, Schwetz T, Winter W (2004) Prospects of accelerator and reactor neutrino oscillation experiments for the coming ten years. Phys Rev D70:073,014, [hep-ph/0403068](#)
36. Huber P, Lindner M, Rolinec M, Winter W (2005) Physics and optimization of beta-beams: From low to very high gamma. Phys Rev D (to be published), [hep-ph/0506237](#)
37. Ioannisian AN, Smirnov AY (2002) Matter effects of thin layers: Detecting oil by oscillations of solar neutrinos [hep-ph/0201012](#)
38. Ioannisian AN, Smirnov AY (2004) Neutrino oscillations in low density medium. Phys Rev Lett 93:241,801, [hep-ph/0404060](#)
39. Ioannisian AN, Kazarian NA, Smirnov AY, Wyler D (2005) A precise analytical description of the earth matter effect on oscillations of low energy neutrinos. Phys Rev D71:033,006, [hep-ph/0407138](#)

- 
40. Itow Y, et al (2001) The JHF-Kamioka neutrino project. Nucl Phys Proc Suppl 111:146–151, [hep-ex/0106019](#)
  41. Jacobsson B, Ohlsson T, Snellman H, Winter W (2002) Effects of random matter density fluctuations on the neutrino oscillation transition probabilities in the earth. Phys Lett B532:259–266, [hep-ph/0112138](#)
  42. Jain P, Ralston JP, Frichter GM (1999) Neutrino absorption tomography of the earth's interior using isotropic ultra-high energy flux. Astropart Phys 12:193–198, [hep-ph/9902206](#)
  43. Kaplan DB, Nelson AE, Weiner N (2004) Neutrino oscillations as a probe of dark energy. Phys Rev Lett 93:091,801, [hep-ph/0401099](#)
  44. Kozlovskaya E, Peltoniemi J, Sarkamo J (2003) The density distribution in the earth along the CERN-Pyhaesalmi baseline and its effect on neutrino oscillations [hep-ph/0305042](#)
  45. Kuo C, Crawford HJ, Jeanloz R, Romanowicz B, Shapiro G, Stevenson ML (1995) Extraterrestrial neutrinos and earth structure. Earth Plan Sci Lett 133:95
  46. Lindner M, Ohlsson T, Tomas R, Winter W (2003) Tomography of the earth's core using supernova neutrinos. Astropart Phys 19:755–770, [hep-ph/0207238](#)
  47. Masters G, Gubbins D (2003) On the resolution of density within the earth. Phys Earth Planet Int 140:159–167
  48. Mikheev SP, Smirnov AY (1985) Resonance enhancement of oscillations in matter and solar neutrino spectroscopy. Sov J Nucl Phys 42:913–917
  49. Mikheev SP, Smirnov AY (1986) Resonant amplification of neutrino oscillations in matter and solar neutrino spectroscopy. Nuovo Cim C9:17–26
  50. Nicolaidis A (1988) Neutrinos for geophysics. Phys Lett B200:553
  51. Nicolaidis A, Jannane M, Tarantola A (1991) Neutrino tomography of the earth. J Geophys Res 96:21,811–21,817
  52. Ohlsson T, Snellman H (2000) Neutrino oscillations with three flavors in matter: Applications to neutrinos traversing the earth. Phys Lett B474:153–162, [hep-ph/9912295](#)
  53. Ohlsson T, Winter W (2001) Reconstruction of the earth's matter density profile using a single neutrino baseline. Phys Lett B512:357–364, [hep-ph/0105293](#)
  54. Ohlsson T, Winter W (2002) Could one find petroleum using neutrino oscillations in matter? Europhys Lett 60:34–39, [hep-ph/0111247](#)
  55. Ohlsson T, Winter W (2003) The role of matter density uncertainties in the analysis of future neutrino factory experiments. Phys Rev D68:073,007, [hep-ph/0307178](#)
  56. Ota T, Sato J (2003) Yet another correlation in the analysis of CP violation using a neutrino oscillation experiment. Phys Rev D67:053,003, [hep-ph/0211095](#)
  57. Petcov ST (1998) Diffractive-like (or parametric-resonance-like?) enhancement of the earth (day-night) effect for solar neutrinos crossing the earth core. Phys Lett B434:321–332, [hep-ph/9805262](#)
  58. Quigg C, Reno MH, Walker TP (1986) Interactions of ultrahigh-energy neutrinos. Phys Rev Lett 57:774
  59. Reynoso MM, Sampayo OA (2004) On neutrino absorption tomography of the earth. Astropart Phys 21:315–324, [hep-ph/0401102](#)
  60. Shan LY, Young BL, Zhang Xm (2002) CP violating neutrino oscillation and uncertainties in earth matter density. Phys Rev D66:053,012, [hep-ph/0110414](#)
  61. Shan LY, et al (2003) Modeling realistic earth matter density for CP violation in neutrino oscillation. Phys Rev D68:013,002, [hep-ph/0303112](#)
  62. Wilson TL (1984) Neutrino tomography: Tevatron mapping versus the neutrino sky. Nature 309:38–42
  63. Winter W (2005) Direct test of the MSW effect by the solar appearance term in beam experiments. Phys Lett B613:67–73, [hep-ph/0411309](#)
  64. Winter W (2005) Geographical issues and physics applications of 'very' long neutrino factory baselines. Nucl Phys B (Proc Suppl) to be published, [hep-ph/0510025](#)
  65. Winter W (2005) Probing the absolute density of the earth's core using a vertical neutrino beam. Phys Rev D72:037,302, [hep-ph/0502097](#)

- 
66. Wolfenstein L (1978) Neutrino oscillations in matter. *Phys Rev D* 17:2369
  67. Zucchelli P (2002) A novel concept for a anti- $\bar{\nu}_e/\nu_e$  neutrino factory: The beta beam. *Phys Lett B* 532:166–172